JOURNAL OF SOLID STATE CHEMISTRY 5, 49–56 (1972)

Thermal Oxidation of Eu_2SiO_4—a Topotactic Solid State Reaction

J. FELSCHE

Institut für Kristallographie der ETH, Zürich, Switzerland

E. KALDIS

Laboratorium für Festkörperphysik der ETH, Zürich, Switzerland

Received August 16, 1971

The appearance of metastable apatite-like phases during the oxidation of Eu_2SiO_4 to Eu_2SiO_5 is discussed in terms of topotaxy. From dta and tga experiments, which are correlated with X-ray single crystal and powder data, the first step in the partial oxidation at 500°C is suggested to be due to the formation of Eu apatite. The silicate apatite crystals show a stoichiometry different from Eu_2SiO_4 and Eu_2SiO_5. However, they contain strings of $[EuO_9]$ polyhedra, which are very similar to the structure of high-Eu_2SiO_4. This favours the reaction towards Eu^{2+} and Eu^{3+} containing apatite I initially. Finally Eu_2SiO_5 is observed above 1000°C after the excess of EuO has been oxidized to Eu_2O_3 and partially incorporated to apatite II.

Introduction

Europium(II)orthosilicate, Eu_2SiO_4, was prepared for the first time by solid state reaction of stoichiometric EuO and SiO_2 quantities in hydrogen atmosphere (*1*). Small crystals grown rather by chance during this synthesis enabled some first physical (*1*, *2*) and crystallographic measurements (*3*). These investigations showed the compound to be ferromagnetic ($T_c = 10°K$) and to have an orthorhombic structure which showed superstructure reflections due to a 7×7.09 Å $\sim$ 49.5 Å superperiod along the *b*-axis (*3*). However, due to the poor reproducibility (*4*) of the crystal growth these investigations could not be further followed.

Recently a new experimental technique, the high-temperature chemical transport (*5*), made the growth of high-quality single crystals of Eu_2SiO_4 possible (*6*). Crystals with dimensions of $4 \times 3 \times 1$ mm were grown by HCl, iodine and bromine transport in sealed Mo crucibles at 2050°C. Magnetic, optical and mass-spectrometric measurements showed that these crystals are very pure and do not contain any Eu^{3+} (*7*). Optical measurements showed that these crystals undergo at 170°C a phase transition (*8*). A crystallographic investigation confirmed these results and showed that Eu_2SiO_4 undergoes a displacive type transition with a change of lattice symmetry from monoclinic to orthorhombic (*8*). The structure of the low temperature form—which is isostructural with β-Ca_2SiO_4—has recently been described (*9*). It was also found (*10*) that the low Eu_2SiO_4 shows an extremely intense luminescence, even at room temperature. Doping with small amounts of Eu^{3+} supresses this property and stabilizes at room temperature the orthorhombic modification (*10*). Therefore, only Eu^{3+}-free crystals show luminescence and phase transition.

During the synthesis of the crystals often complicated X-ray powder-diffraction patterns were observed for Eu^{3+}-rich, slightly oxidized phases. It was decided, therefore, to investigate the oxidation of Eu_2SiO_4 in oxygen or air using pure monoclinic crystals as starting materials. The results of this investigation are presented in this paper. The oxidation reaction has been studied between 300 and 1550°C by simultaneous dta and tga runs on a Mettler thermobalance. Starting and resulting products have been examined by X-ray single crystal and powder methods.

Results

The crystals of Eu_2SiO_4 used for the oxidation experiments have been grown by high-temperature chemical transport at 2050°C in a sealed

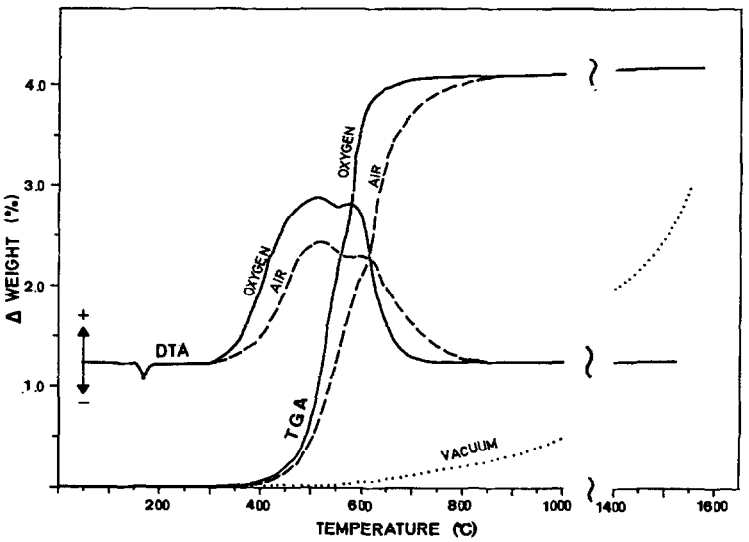

FIG. 1. Thermal behaviour of Eu_2SiO_4 under dried oxygen, air (760 mm Hg) and high vacuum ($10^{-6} \rightarrow 10^{-4}$ mm Hg) in dta and tga experiments. Heating rate, 4°C/min; starting weight, 15.4 mg Eu_2SiO_4.

Mo crucible using HCl as transporting agent. The total impurity content in these crystals of Cl, Al, Ca, La, Mg, K and other elements was less than 400 ppm (weight) (*7*). They showed monoclinic symmetry of space group $P2_1/n$ on the precession camera. Cell dimensions are $a = 5.65$ Å, $b = 7.09$ Å, $c = 9.76$ Å and $\beta = 92.6°$ as already reported in (*8*, *9*).

A fine grained powder of this material with maximum particle size of 5 μ was used for several dta/tga runs under different conditions starting with about 15 mg in each experiment. In Fig. 1 the course of the reaction up to 1550°C under different atmospheres is given as reproduced from the recorder strips (4°C/min, 15.4 mg Eu_2SiO_4). On the dta tracings the transition from monoclinic to orthorhombic is clearly indicated by an endothermic peak at 170°C in agreement with the former results (*8*). Allowing purge gas flow of 10 liter/hr of dried oxygen and air at normal pressure the oxidation starts at about 300°C with an appreciable delay in weight change (370°C) compared to the dta signal. The two maxima of the exothermic dta peak at 500°C/580°C in oxygen and 500°C/620°C in air suggest some evidence of two successive types of reaction of the material. An analogous discontinuity in the tga-slope can also be observed after about 70% gain of weight. The oxidation appears to be completed at about 750 and 850°C in oxygen and in air, respectively, corresponding to a total gain of weight of 4.0 ± 0.1% of the starting material, Eu_2SiO_4 in both cases (theoretical value of $\Delta G = 4.1$%.)

It should be mentioned, however, that the weight loss temperature relationship given in Fig. 1 is strongly correlated to the heating rate of 4°C/min. Static experiments (24 hr per fixed temperature) showed with high reproducibility that the oxidation in air starts at about 250°C (±20°C) and is finished at about 350°C (±20°C). This time dependency shows that the oxidation of Eu_2SiO_4 is kinetically controlled.

X-Ray powder examination of the oxidized crystals revealed a surprising result. FeK_α Guinier photographs showed an apatite phase of the material when quenched from 600–1000°C after the oxidation had been completed according to the dta–tga signal. The phase which actually would have been expected from the oxidation following the formal equation

$$Eu_2SiO_4 + 1/2O_2 \rightarrow Eu_2SiO_5$$

could, however, not be observed by X-ray techniques at specimens annealed below 1100°C. Long time heating experiments (>20hr) above 1100°C only provided sufficient crystallinity of the Eu_2SiO_5 phase to be detectable for X-rays. The quenched apatite-like material also showed only a very weak and diffuse X-ray powder pattern. An analysis of the line width gave values for the particle size of 800 ± 100 Å. The particle size could be increased however by long time heating experiments to about 4000 Å. This

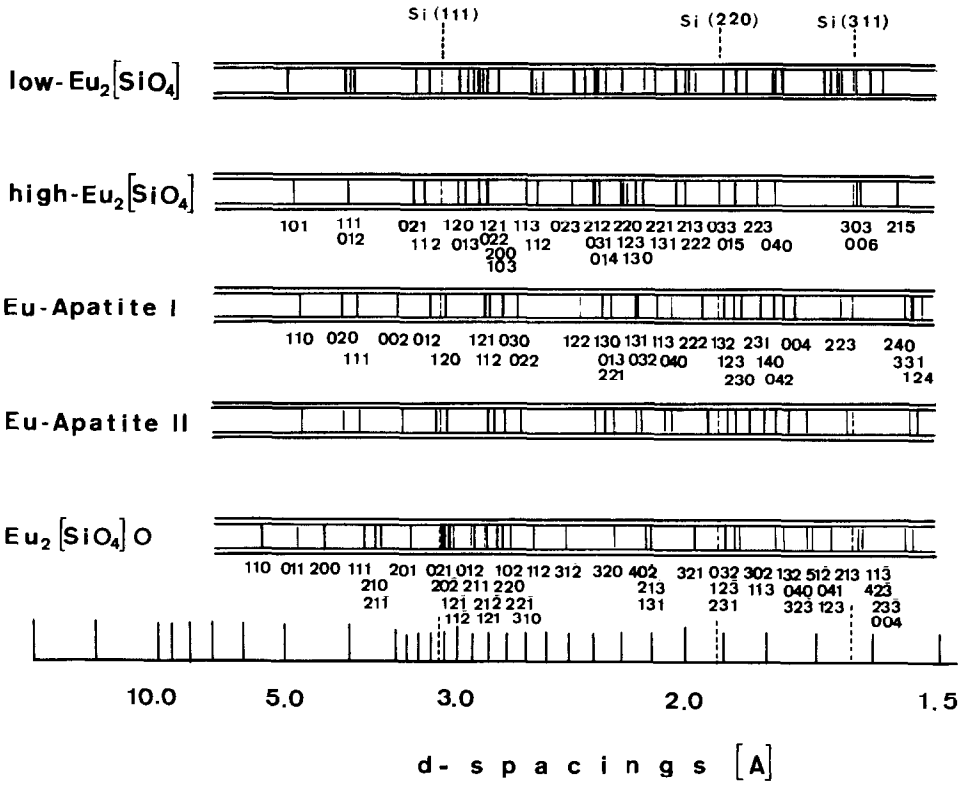

FIG. 2. X-ray powder patterns of crystalline phases as observed during the oxidation of Eu_2SiO_4. For comparison see Table I. Main interferences copied from Guinier FeK_α photographs in the scale 1:1.33. Indexing based on data from Table I with low-$Eu_2[SiO_4]$ in the setting of $P2_1/n$.

allowed a better interpretation of the X-ray pattern. Annealing of the specimens at temperatures of 600–750°C in dry air or oxygen resulted in an apatite phase with cell dimensions $a = 9.47 \pm 0.02$ Å and $c = 6.99 \pm 0.02$ Å. In the temperature range of 750–1000°C a smaller cell volume was observed with $a = 9.47 \pm 01$ Å and $c = 6.89 \pm 0.01$ Å. At higher temperatures $1000°C < T < 1100°C$ mixed phases with Eu_2SiO_5 were found. Indexed powder patterns are given in Fig. 2.

These results were confirmed by corresponding single crystal X-ray experiments. On a heating precession camera the phase transition from monoclinic to orthorhombic was indicated first at about 170°C. Using a platelike crystal ($0.1 \times 0.2 \times 0.2$ mm) the successive reaction of the crystal on higher temperatures was followed at the *h0l* and *hk*0 reciprocal lattice planes alternatively. The documentation of the speedy process was possible by time-saving employment of Polaroid type 57 films (5 min exposure) using MoK_α radiation for 15°-precession-angle photographs. Stepwise elevating the temperature and taking photographs of the specimen at constant temperatures from 300 to 1500°C showed the following results.

The first reaction of the single crystal was indicated by the disappearance of the weak reflections *h0l* and *hk*0 and later on by increasing diffuseness of the strong reflections (103), (200) and 120). Before they had completely disappeared at about 600°C already (120) and (121) powder interferences of the apatite-like phase could be observed on the same photograph. At temperatures higher than 1000°C the apatite pattern was replaced by Eu_2SiO_5 interferences accordingly.

Discussion

The appearance of the rare earth apatite as an intermediate phase during the oxidation of Eu_2SiO_4 needs some detailed discussion. This phase is unexpected from the stoichiometry of the oxyapatites which is quite different from that

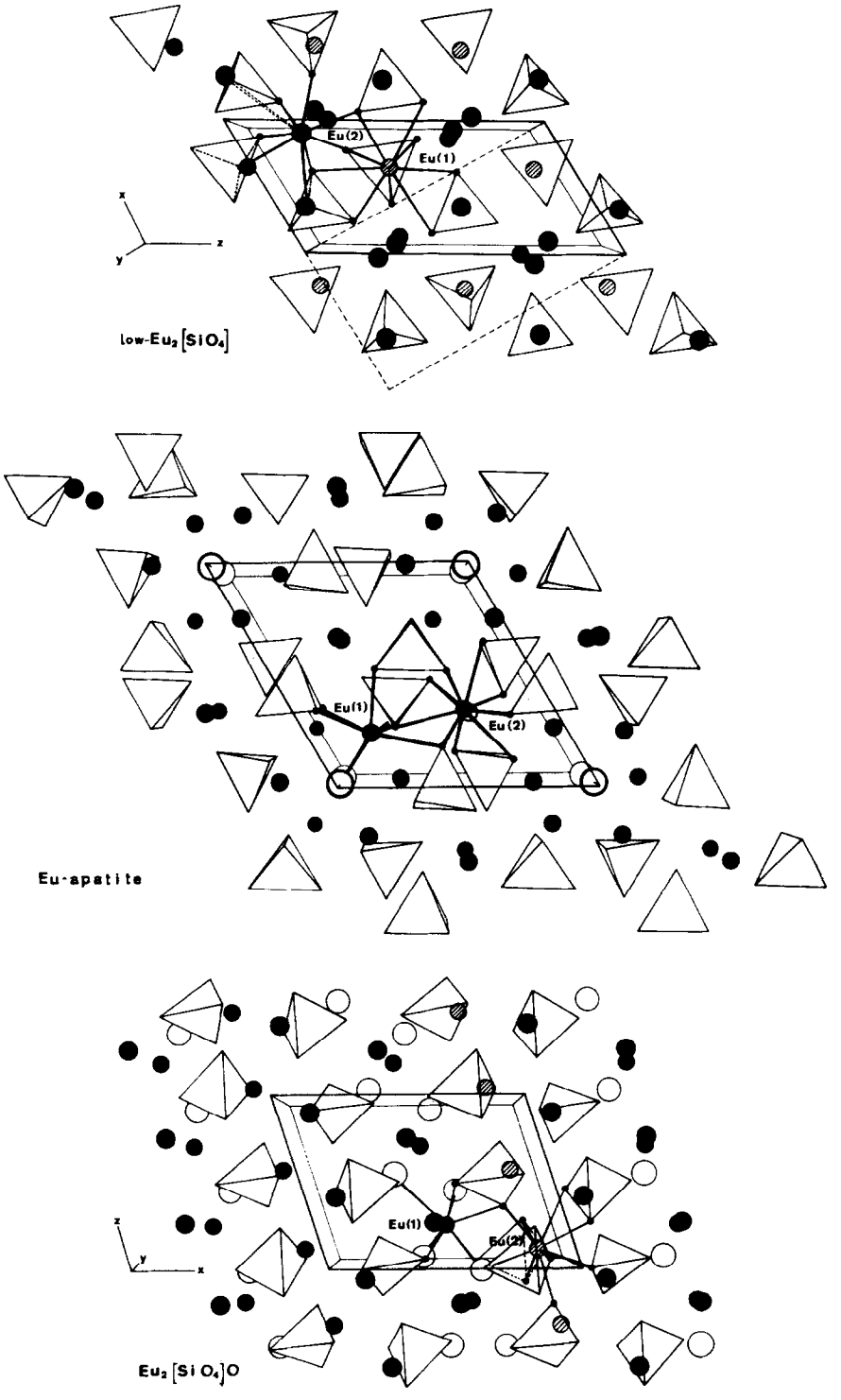

FIG. 3. Perspective view of the crystal structures of phases as observed during the oxidation of Eu_2SiO_4. For comparison see data in Table I. Low-$Eu_2[SiO_4]$ is given in the setting of $P2_1/c$ (*9*); $P2_1/n$ is indicated by dashed cell outline. The 9-fold oxygen coordination of Eu(*2*) in the closely related structure of high-Eu_2SiO_4 is indicated by the additional dashed-line stick. Eu apatite I/II data from (*12*), $Eu_2[SiO_4]O$ data from (*16*). Black balls: Eu atoms; large circles: "extra (not silicon bonded) oxygens"; solid $[SiO_4]$ tetrahedra.

of the starting compound Eu_2SiO_4 ($2EuO \cdot SiO_2$) and the final oxidation product Eu_2SiO_5 ($Eu_2O_3 \cdot SiO_2$). Two types of europium apatites are known. First the binary compound $7Eu_2O_3 \cdot 9SiO_2$. The structure shows a cation deficiency in the 9-fold coordinated (4*f*) position of Eu(2) due to $(Eu_{3.33}\square_{.66})^{[9]}Eu_6^{[7]}[SiO_4]_6O_2^{[3]}$ ([*n*] gives coordination number). This was first argued from an investigation of La apatite (*11*) and later also confirmed for the Gd analogue (*12*). From corresponding X-ray powder patterns this apatite structure was assumed to exist for nearly all rare earths (*12, 13*). This is a remarkable feature in the field of rare earth oxide compounds since there is no other binary phase known so far which exists in only one modification for such a large number of trivalent rare earths. Obviously the apatite structure type represents an extremely favourable atomic arrangement tolerant for all larger cation and complex anion charge coupled substitution.

There is a second type of europium apatite which contains divalent and trivalent cations as well of composition $2EuO \cdot 4Eu_2O_3 \cdot 6SiO_2$ (*13*). This structure shows a larger cell volume due to an elongation of the *c*-axis. It contains 10 europium ions in the unit cell as compared to 9.33 Eu^{3+} ions in the other structure. The cation distribution on the (4*f*) and (6*h*) lattice sites (Eu(2) and Eu(1) in Fig. 3, respectively) is likely due to $(Eu_2^{2+}, Eu_2^{3+})^{[9]}\ Eu_6^{3+[7]}\ [SiO_4]_6O_2^{[3]}$ (*13*).

It will be shown from structural arguments that both the apatite phases are highly qualified to be formed during the process of oxidation of Eu_2SiO_4. For comparison all three structure types under discussion are represented in Fig. 3 in a perspective view along corresponding crystallographical directions. The crystal data are given in Table I. The basic structure of low-Eu_2SiO_4 needs a little correction since the [SiO_4] tetrahedra get a slight tilt against each other during the displacive transformation at 170°C. In high-Eu_2SiO_4 the relative position of cations and anions remains almost unchanged. The coordination number (CN) of Eu(2) is increased from 8 to 9 because of the tilting of the tetrahedra; CN 10 of Eu(1) is consistent. This description of orthorhombic high-Eu_2SiO_4 is based on data from a recent discussion of phase transformation of the isostructural dicalcium-silicate polymorphs β-$Ca_2SiO_4 \rightarrow \alpha_L \rightarrow, \alpha_H$-$Ca_2SiO_4$ (*14*). A close structural relationship between low- and high-Eu_2SiO_4 had also been

TABLE I

CRYSTAL DATA OF PHASES OBSERVED DURING THE OXIDATION OF Eu_2SiO_4

Compound	Composition	Structural Formula	Unit cell dimensions a (Å)	b (Å)	c (Å)	α, β, γ (°)	Space Group	V [Å^3]	Z	Ref.
low-Eu_2SiO_4	$2EuO \cdot SiO_2$	$Eu^{[8]}Eu^{[10]}[SiO_4]$	5.65	7.09	9.76	92.6	$P2_1/n$	391.1	4	(8)
			5.65	7.09	11.51	122.0	$P2_1/c$	391.1	4	(9)
high-Eu_2SiO_4	$2EuO \cdot SiO_2$	$Eu^{[9]}Eu^{[10]}[SiO_4]$	5.66	7.14	9.77	90.0	$Pmnb$ $P2_1nb$	394.9	4	(8)
Eu apatite I	$2EuO \cdot 4Eu_2O_3 \cdot 6SiO_2$	$(Eu^{2+}, Eu^{3+})_4^{[9]}Eu_6^{[7]}[SiO_4]_6O_2^{[3]}$	9.47	9.47	6.99		$P6_3/m$	542.8	1	(*13*)
Eu apatite II	$7Eu_2O_3 \cdot 9SiO_2$	$(Eu_{3.33} + \square_{.66})^{[9]}Eu_6^{[7]}[SiO_4]_6O_2^{[3]}$	9.47	9.47	6.91		$P6_3/m$	537.0	1	(*12, 13*)
Eu_2SiO_5	$Eu_2O_3 \cdot 2SiO_2$	$Eu^{[9]}Eu^{[7]}[SiO_4]O^{[4]}$	9.15	7.08	6.76	107.83	$P2_1/c$	417.9	4	(*16, 17*)

suggested from the subgroup relation of their space groups $P2_1/n$–$Pmnb$ and the very weak transformation of the displacive type as observed during former experiments (*8*).

Obviously it is the extremely similar 9-fold coordination of Eu(2) in Eu_2SiO_4 and the Eu apatite which favours the formation of the oxy-apatite structure. Both the europium ions are surrounded by 6[SiO_4) tetrahedra. Both show coordination numbers 9 with average Eu–O bond lengths of about 2.55 Å (*9*) and 2.53 Å (*12*), respectively. Three of the nine bonds are directed to the corners of three isolated tetrahedra while the remaining six point towards three tetrahedra edges. Columns of these polyhedra from Eu_2SiO_4 may be retained unchanged without breaking of Eu–O bonds for the formation of the apatite structure. The apatite structure on the other hand can be regarded as being built up of these columns along the 6-fold rotary-inversion axis plus additional europium cations and single oxygen ions arranged in the wide channels left between along the 6_3-screw axis. Thus the transformation from Eu_2SiO_4 to Eu apatite might be considered to be of the semireconstructive type in the terminology of Buerger (*15*).

However, there is one point resulting from the different stoichiometry which opposes this simple analysis of geometrical features. As can be seen from the data in Table II there is an excess of 1/6 of the total europium concentration when going from Eu_2SiO_4 to Eu apatite I. This has to be removed from the structure while two oxygens have to be inserted into the new apatite-like arrangement. It is possible that this excess of europium at the crystalline interfaces keeps the apatite particle size down to about 4000 Å as observed during the long time thermal treatment of the material.

The exothermic double peak in the dta experiments is in agreement with this hypothesis. The first maximum is due to the oxidation of 8/12 of the europium ions. These are accommodated in the apatite unit cell in addition to the 2/12 Eu^{2+} ion whose valency remains unchanged for the apatite I structure. Thus the first step of the partial oxidation is characterized by the structural integration of two oxygens. Two additional oxygens are necessary for charge balance of the two excessive Eu^{2+} ions.

The second maximum of the exothermic dta signal at 580°C and 620°C, in oxygen and in air, respectively, arises from the oxidation of the remaining 4/12 Eu^{2+} ions present in the apatite I structure and the Eu monoxide. The oxidized trivalent europium is partially used for the formation of the apatite II phase at elevated temperatures. The rest of it might exist in the form of Eu_2O_3 at the apatite grain boundaries. If crystalline clusters of Eu_3O_3 could be present at all in the bulk they must have a particle size <500 Å since no Eu_2O_3, Eu_3O_4 or EuO had ever been observed on the X-ray powder photographs besides the silicate phases. This interpretation in terms of partial oxidation directed by the topotactic reaction of the Eu_2SiO_4 structure is consistent also with the tga result: The discontinuity in the slope of the tga curve in Fig. 1 occurs just after about 2/3 of the total gain of weight.

At temperatures above 1000°C the apatite structure becomes unstable and it is replaced successively by the oxyorthosilicate $Eu_2[SiO_4]O$ which incorporates the dispersed Eu_2O_3. This structure type has recently been determined for the Gd analogue (*16*). It is known to exist for all larger rare earths La–Tb (*16*, *17*). As in the apatite structure the heavy atoms are 7- and 9-fold oxygen coordinated. But the amount of "extra (not Si-bonded) oxygens" is enlarged. Thus the structural arrangement must be different. It is also evident already from the different surroundings of the rare earth cations. There are four "extra oxygens" present in the 7-fold coordination of Eu(1) and one in the first coordination shell of Eu(2) with CN 9. The higher value for the ratio $Eu:O_{ex}$ in $Eu_2[SiO_4]O$ is also responsible for the different *cation*-coordination around these "extra oxygens." Four europium cations (3 Eu(1) + 1 Eu(2)) surround the "extra oxygen" in $Eu_2[SiO_4]O$ in the shape of a slightly distorted tetrahedron while there are only three Eu(1) ions next neighbours of the "apatite oxygen" positioned at the corner of a triangle. The sheet-like packing of [O Eu_4] and [SiO_4] tetrahedra parallel (100) demonstrates best the strong dissimilarity to both the Eu apatite and Eu_2SiO_4 structure. From this it is best understood that the energy barrier between Eu_2SiO_4 and $Eu_2[SiO_4]O$ favours the formation of the apatite phase.

It should be noted that a similar behaviour of the europium(II)oxide on thermal treatment has recently been reported (*18*). After a partial oxidation of EuO, Eu_3O_4 is formed as the intermediate phase due to

$$6EuO \xrightarrow[420°C]{O_2} 2Eu_3O_4 \xrightarrow[503°C]{+O_2} 3Eu_2O_3$$

TABLE II

PHASE RELATIONS AND CHANGES IN STOICHIOMETRY DURING THE OXIDATION OF Eu_2SiO_4

	Cryst. Phases from X-ray Exam.	Σ Mol. under Comparison	Ions per unit cell volume $\cdot(n)$ of Cryst. Phases	Cell Volume $\cdot(n)$	Σ Mol. Weight
	$Eu_2[SiO_4]$ (-high)	$12EuO \cdot 6SiO_2$	$12Eu^{2+} + 6[SiO_4]^{-4}$	592.5 Å^3 (1.5)	2328.1
Step I (500°C–Ox.)		$+2O_2$	$-2Eu^{2+} + 2O^{2-}$	$-\Delta V = 49.5$ Å^3	$+\Delta W = 2.75\%$
	Apatite I	$2EuO \cdot 4Eu_2O_3 \cdot 6SiO_2 +$ 2EuO	$2Eu^{2+} + 8Eu^{3+} + 6[SiO_4] + 2O^{2-}$	543.0 Å^3 1.0	2392.1
Step II (580°C–Ox.)		$+1O_2$	$-2/3Eu^{2+}$	$-\Delta V = 9.0$ Å^3	$+\Delta W = 1.35\%$
	Apatite II	$4\frac{2}{3}Eu_2O_3 \cdot 6SiO_2 +$ $1\frac{1}{3}Eu_2O_3$	$9\frac{1}{3}\ Eu^{3+} + 6[SiO_4] + 2O^{2}$	537.0 Å^3 1.0	2424.0
Step III (T>1000°C)			$+2\frac{2}{3}Eu^{3+} + 4O^{2-}$	$+\Delta V = 90.0$ Å^3	$\Delta W = 0$
	$Eu_2[SiO_4]O$	$6Eu_2O_3 \cdot 6SiO_2$	$12Eu^{3+} + 6[SiO_4]^{-4} + 6O^{2-}$	627.0 Å^3 (1.5)	2424.0

before *B*-type Eu_2O_3 appears as the final product of oxidation. As suggested from the more complex character of the silicate structure the final oxidation of the simple europium monoxide occurs at lower temperatures.

Acknowledgments

The authors thank Prof. G. Busch and Prof. F. Laves for their interest in this work and Mr. R. Bachmann and W. Hirsiger for their technical assistance.

References

1. M. W. SHAFER, T. R. MCGUIRE, AND J. C. SUITS, *Phys. Rev. Lett.* **11**, 251 (1963).
2. M. W. SHAFER, *J. Appl. Phys.* **36**, 1145 (1965).
3. R. C. RAU, *Acta Crystallogr.* **17**, 1483 (1964).
4. M. W. SUITS, B. E. ARGYLE, AND M. J. FREISER, *J. Appl. Phys.* **37**, 1391 (1966).
5. E. KALDIS, *J. Cryst. Growth* **9**, 281 (1971).
6. E. KALDIS, *Z. Kristallogr. Kristallgeometrie, Kristallphys. kristallchem.* **128**, 444 (1969).
7. E. KALDIS AND R. VERREAULT, *J. Less Common Metals* **20**, 177 (1970).
8. G. BUSCH, E. KALDIS, R. VERREAULT, AND J. FELSCHE, *Mat. Res. Bull.* **5**, 9 (1970).
9. J. FELSCHE, *Naturwissenschaften* **4**, 218 (1971).
10. E. KALDIS, P. STREIT, AND P. WACHTER, *J. Phys. Chem. Solids* **32**, 159 (1971).
11. E. A. KUZ'MIN AND N. V. BELOV, *Sov. Phys. Dokl.* **10**, 1009 (1966).
12. YU. I. SMOLIN AND YU. F. SHEPELEV, *Isv. Akad. Nauk SSSR Neorg. Mat.* **5**, 1823 (1969).
13. J. FELSCHE, *J. Solid State Chem.* (in the press 1972).
14. W. EYSEL AND TH. HAHN, *Z. Kristallogr. Kristallgeometrie, Kristallphys. Kristallchem.* **131**, 322 (1970).
15. M. J. BUERGER, *Amer. Mineral.* **33**, 101 (1948).
16. YU. I. SMOLIN AND S. P. TKACHEV, *Sov. Phys. Cryst.* **14**, 14 (1969).
17. J. FELSCHE, *Naturwissenschaften* **58**, 565 (1971).
18. N. I. IGNAT'EVA AND V. G. BAMBUROV, *Isv. Akad. Nauk SSSR, Neorg. Mat.* **6**, 154 (1970).